

LIQUID PHASE VELOCITY IN TURBULENT FLOW OF A WATER/DISPERSED BUBBLE MIXTURE IN LARGE DIAMETER HORIZONTAL PIPES

A. A. Lakis* and N.D.Trinh

Department of Mechanical Engineering, École Polytechnique de Montréal. C.P. 6079, Succ. Centre-Ville, Montréal, Québec, CANADA H3C 3A7.

*Corresponding author: aouni.lakis@polymtl.ca

ABSTRACT

Methods for the measurement of impact pressure in two-phase bubble flow are discussed, leading to the design of a liquid phase isolator. This simple device, equipped with a miniature pressure transducer, makes it possible to measure the impact pressure of the liquid phase in a flowing gas-liquid mixture. The liquid velocity can then be predicted, provided that the local void fraction is known. Using a measured void fraction it is possible to predict the pressure drop, mixture and phase velocities, and liquid phase distribution by either finding new correlations or using a newly-developed numerical model. Experiments were performed in 8.6-in (218.44 mm) diameter horizontal pipes with 0.30 maximum flow volumetric qualities. In high turbulence conditions ($Re = 2 \times 10^6$), we observed that the liquid velocity profile behaves like single-phase liquid flow; the symmetry of the profile changes when flow volumetric quality varies from about 12 % to its maximum value. It was determined that, in fully-developed dispersed bubble flow the void fraction is uniform, giving rise to a uniform vertical pressure distribution. This strongly influences the vertical phase distribution. The liquid velocity distribution was found to be uniform in the vertical plane. The presence of a large concentration of bubbles in the upper part of the pipe causes the velocity of the liquid there to be generally lower than in the liquid phase; the liquid velocity decreases in the transversal plane because of the drag effect of local displaced bubbles. Liquid velocity is therefore distributed non-uniformly in the transversal plane. The effects of gravity (assuming it to be stabilized in steady fully developed flow), interfacial forces and the turbulence structure of the continuous phase appear to have a great influence on the liquid phase velocity distribution in a large horizontal pipe. In this study, the liquid phase velocity of turbulent flow of a water/dispersed bubble mixture in large diameter pipes is predicted. The first step is development of a measuring technique for the liquid phase velocity of dispersed bubble flow. Subsequently, the relationship between the phase distribution mechanism and the turbulence structure in the continuous phase is expressed in terms of linear liquid velocities (in single-phase and two-phase flows). Finally, velocity distributions determined using experimental data are compared with those predicted numerically.

Keyword: Two-phase bubble flow, liquid phase velocity and large diameter horizontal pipe flow.

INTRODUCTION

Liquid velocity plays an important role in the physical modeling of both single and two-phase flow. If a liquid is the continuous phase of a flowing mixture, knowledge of its velocity distribution permits a better understanding of the turbulence structure of the flow and the phase distribution mechanism.

The linear velocity of the liquid in gas-liquid mixture flow may be determined in the same way as in single-phase liquid flow. Methods currently used include injecting a solution into the flow and measurement of the transit time of fluid particles between two successive electrodes (Sodium chloride, Jepsen and Ralph; salt water or hot water, Kinoshita and Murasaki, Serizawa *et al.*), or measurement of the oxygen reduction velocity at the surface of the electrodes. This velocity varies with that of the flow (electrochemical method, Mitchell and Hanratty; electrodiffusion, Kozmienko *et al.*, Nakoryakov *et al.*, Kashinsky *et al.*, and Pannek *et al.*). The $1/6$ to $1/7$ power law found in the turbulent case indicates that the profiles are very close to those noted in turbulent single-phase flow.

Using an isokinetic sampling method (the static pressure is equalized at the entrance of the probe and at the same axial position in the flow), Alia *et al.*, Jepsen and Ralph, showed that the liquid velocity of a bubbly flow with an annular entrance/mixing section may be deduced from pressure, mass flow rate and void fraction data.

The signal analysis method proposed by Delhaye, Serizawa *et al.*, and Galaup was used to obtain the liquid velocity with a hot film anemometer and the amplitude histogram from a multichannel analyzer. A power law of $1/7$, obtained with Laser Doppler velocimetry, was reported in Ohba *et al.* and Vassallo *et al.*, for liquid velocity distribution in vertical upward/downward bubble flow. Brown *et al.*, assume that the liquid velocity profile can be represented by a parabolic function to which a correction factor varying from zero to one is applied.

Minemura *et al.* present the liquid velocity as a potential for a quasi-harmonic equation. This equation is solved using the finite element method to obtain the velocities, and the equation of motion of an air bubble is integrated numerically into the flow field to obtain the void fraction.

The numerical model of Sato and Seroguchi, verifies experimental work carried out in a vertical rectangular tube of 25 x 50 mm. The shear stress of the liquid phase (air-water flow) is separated into two parts: one related to the inherent turbulence of the liquid independent of the existence of the bubbles, the other to the supplementary turbulence of the liquid caused by bubble agitation. Bankoff *et al* proposes a power law distribution for each velocity and void fraction profile, where the shear stress is presumed to be uniform over all sections of the pipe.

Brown and Kranich, on the other hand, propose a logarithmic distribution for the velocity of air-water bubble flow. Krashcheev and Muranov calculate the velocity of a bubbly flow with an annular entrance/mixing section by replacing the flow by a homogeneous medium; shear stress and the core film interface velocity are of the same order of magnitude. Prandtl's mixing length theory is applied by Bankoff *et al*, Levy *et al*, and Gorin *et al* for analytical treatment of velocity distribution.

In this work, the void fraction of dispersed bubble flow in a large diameter horizontal pipe is predicted. During our investigation, we first develop a technique for measuring the liquid phase velocity of dispersed bubble flow (Morgan *et al.* 2016). Secondly, the relationship between the phase distribution mechanism and the turbulence structure in the continuous phase is expressed in terms of linear liquid velocities (in single- phase and two-phase flows) and the measured void fraction (Lakis, A. A., *et al* (1988)). Finally, velocity distributions determined using experimental data are compared with those predicted numerically. The numerical work is based on the model proposed by Sato and Seroguchi for bubble flow.

Description of the experiment

The horizontal air-water flow facility is shown schematically in Figure 1. This facility was installed and used by Lakis (1978) for studying wall pressure fluctuations in annularly dispersed bubble flow.

Water flows from a 15000 USG (55500 liters) open reservoir through the circuit at a rate of 2000 to 5000 USGPM (7400 to 18500 l) and is mixed with compressed air to produce a two-phase flow. Experiments were conducted in a series of horizontal pipes of 8.6 in (218.44 mm) nominal diameter located at “130 diameters” total distance from the mixer. Pipelines consisted of interchangeable PVC pipes, a steel pipe (for installing the wall pressure transducers), and a Plexiglas pipe (thickness: 0.975 in (24 mm) and internal diameter 7.625 in (193.68 mm)). Evolution of the flow can be visually monitored by moving the clear section along the pipe (Sookhak Lari, K. *et al.*, 2013).

The friction velocity in two-phase flow was evaluated from pressure drop measurements made with Bourdon-type pressure transducers which are connected to pressure taps located along the pipe.

Due to the limited capacity of the piping circuit, the maximum flow volumetric quality (ratio of gas volumetric flow rate to total volumetric flow rate) was 30 %. The following three observable flow regimes were obtained: slug flow, dispersed slug waved flow and stratified dispersed bubble flow as shown in Figure 2.

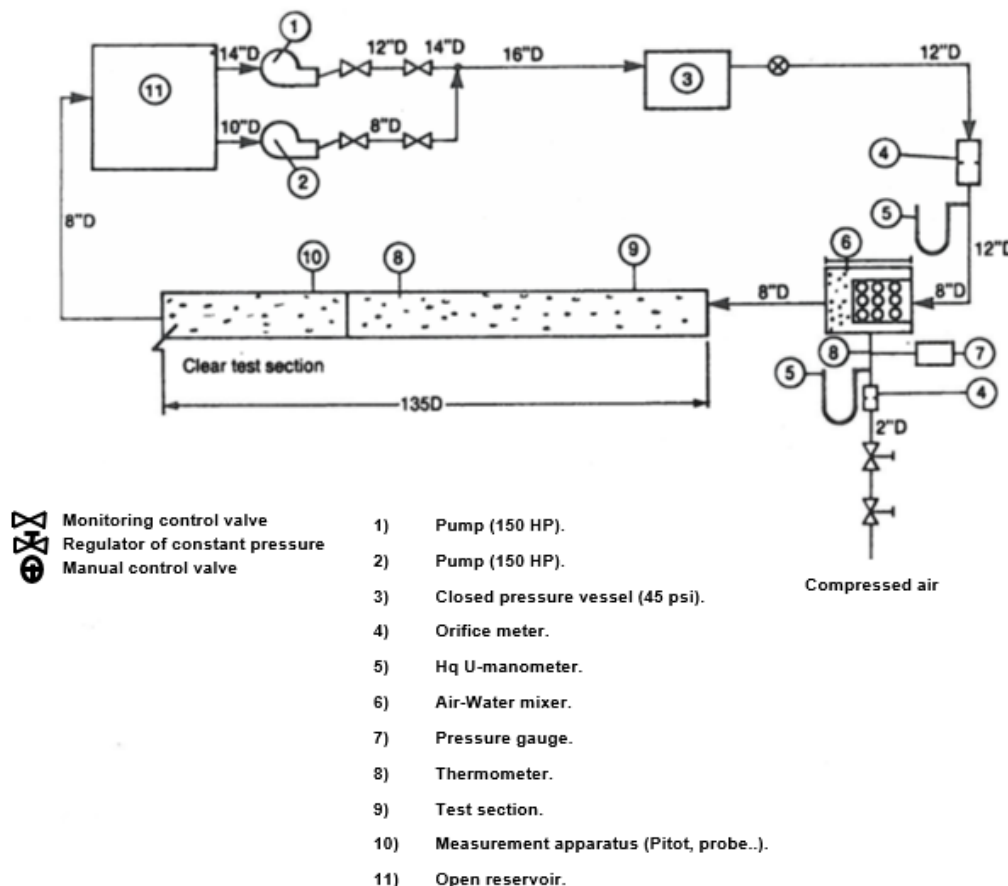


Figure 1: Horizontal test loop.

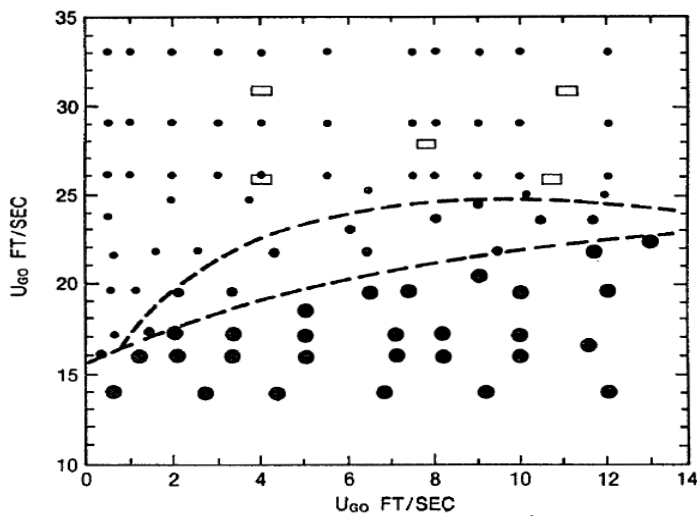


Figure 2 Flow map of horizontal air-water flow. (8-in. nominal diameter, fully developed flow $z/D = 130$)

- Slug flow
- Dispersed slug waved flow
- Stratified - dispersed bubbles flow
- Values chosen for experimentation
- Transition zones.

Figure 2: Flow map of horizontal air-water flow. (8.6-in (218.44 mm) nominal diameter, fully-developed flow $z/D=130$).

The experimental conditions summarized in Table 1 clearly refer to the case of stratified dispersed bubble flow.

Table 1: Experimental conditions

AIR			WATER		
$T_G = 24^\circ \pm 2^\circ\text{C}, P_G = 50 \text{ PSIG}, \rho_G = 0.255 \text{ lbm/ft}^3$			$T_L = 19^\circ \pm 2^\circ\text{C}, P_L = 1 \text{ ATM}, \rho_L = 62.4 \text{ lbm/ft}^3$		
			$\nu_L = 1.088 \cdot 10^{-5} \text{ft}^2/\text{sec}$		
$Q_{Go}(\text{ft}^3/\text{min})$	$U_{Go}(\text{ft}/\text{sec})$	X_o	$Q_{Lo}(\text{USGPM})$	$U_{Lo}(\text{ft}/\text{sec})$	
76.6	4.03	.116	4373	30.74	
73.8	3.88	.131	3666	25.77	
147.6	7.76	.219	3940	27.69	
209.8	11.03	.264	4373	30.74	
202.2	10.63	.292	3666	25.77	

$$X_o = \frac{Q_{Go}}{Q_{Go} + Q_{Lo}}, \alpha_{Go} = 19.02 * U_{Go}, Q_{Lo} = 142.26 * U_{Lo}, \rho_G = \frac{2.698 * (\text{PSIG})}{459.69 + ^\circ\text{F}}$$

ID = 7.625 in, $Re_L(\text{max}) = 2 * 10^6$, Mach (max) = 0.014 (<0.2, incompressible)

Entrance ($Z/D = 0$)

Exit ($Z/D = 170$)

* 24 Axial locations

* 9 Radial positions (Transversal plane A and Radial plane B)

Experimental measurements were made and numerical analyses were carried out for fully-developed flow conditions. More detail on experimental apparatus and procedure may be found in Trinh *et al.*, 1986.

Principle of measurement of local liquid phase velocity

Use of Pitot tube and pressure transducers

The use of Pitot tube and differential pressure transducers in two-phase flow has been adopted by several investigators, notably Halbronn, Gill *et al.* for studying annularly dispersed flow (Dispersed flow is characterized by the flow where one phase is dispersed in the other continuous phase.) Kinoshita and Murasaki for analysing pulsating phenomena, Zigami *et al.* for measuring liquid phase variables, Fincke and Deason, Lakis and Mohamed for experimenting with dispersed bubble flow, etc.

The presence of the dispersed phase in a continuously flowing mixture is characterized by the proportion occupied by this phase along the flow. In air-water mixture flow, this proportion represents the quasi-static fraction of air bubbles and is symbolized by α . Since the void fraction is a measure of the change in proportion resulting from either a variation in the dispersed phase or interaction between the phases, it represents an additional independent kinetic variable in the general expression for two-phase flow.

In general, the interpretation of measured impact pressure is difficult unless the measured variable is well specified. The isokinetic sampling method was adopted by Anderson and Manzouranis for studying the flow with air predominating, and by Jespen and Ralph, Shires and Riley, Alia *et al.*, in obtaining information about one phase in an annularly dispersed flow.

The use of a Pitot tube in two-phase flow is efficient when its opening diameter is considerably smaller than that of the bubbles. However, using a small diameter Pitot tube increases the duration of the measuring time. If the Pitot tube is large enough for bubbles to enter, the presence of bubbles in the tube or in the connecting lines leads to erroneous pressure readings. The method adopted for this study is the use of a current of water under pressure with a set of three nozzle taps in which the flow remains constant in the direction of the manometer tap. Another approach suitable for this study is an air current constantly flowing in the direction of the manometer pressure taps at a given pressure. The current must be adjusted automatically in order to maintain equilibrium with the pressure used during the experiment. The difference between initial and final values represents the desired total pressure Chen, K.S. *et al* (2001).

In this investigation, the average impact pressure of the two-phase flow is initially determined using a Pitot tube with a diaphragm-type differential pressure transducer. Air is purged in two clear cylindrical containers which are always filled with water before entering both sides of the pressure transducer. Air bubbles can later be freely evacuated to the atmosphere by means of a valve situated on the top of each container or air-purger.

A schematic diagram of the measuring system is shown in Figure 3.

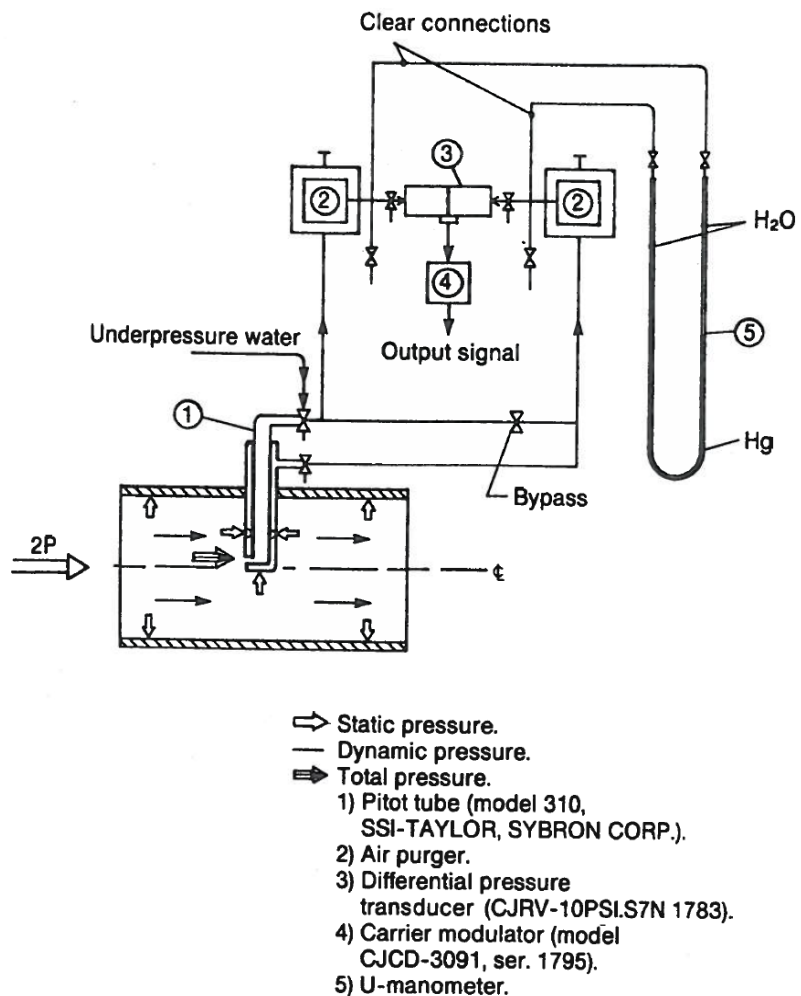


Figure 3: Measurement of dynamic pressure in two-phase flow with a Pitot tube and differential pressure transducer.

Unfortunately, this method proved unsuccessful in making reliable measurements during experimentation due to the presence of bubbles, which accumulate in the measurement system after a relatively short period. In addition, use of the water current under pressure could not guarantee the absence of bubbles in the Pitot tube itself in the higher range of flow volumetric quality.

Isolation of liquid in two-phase gas-liquid flow

Assuming that pressure signals obtained at a stagnation point result uniquely from the liquid phase, the measured velocity will be that of the liquid phase in the mixture. In order to obtain meaningful measurements, we wish to minimize the kinetic energy of the gas phase at this point without disturbing the dynamic behavior of the liquid phase.

A so-called liquid isolator has been designed for this purpose. By mounting this isolator on a miniature differential pressure transducer, the air bubbles are eliminated at the stagnation point. The rectilinear opening of the isolator is in contact simultaneously with the pressure-sensitive area of the transducer and with the surrounding fluid.

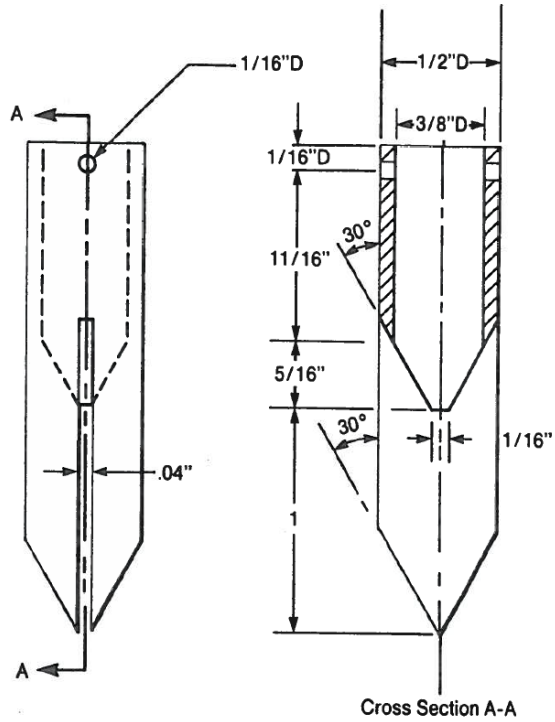
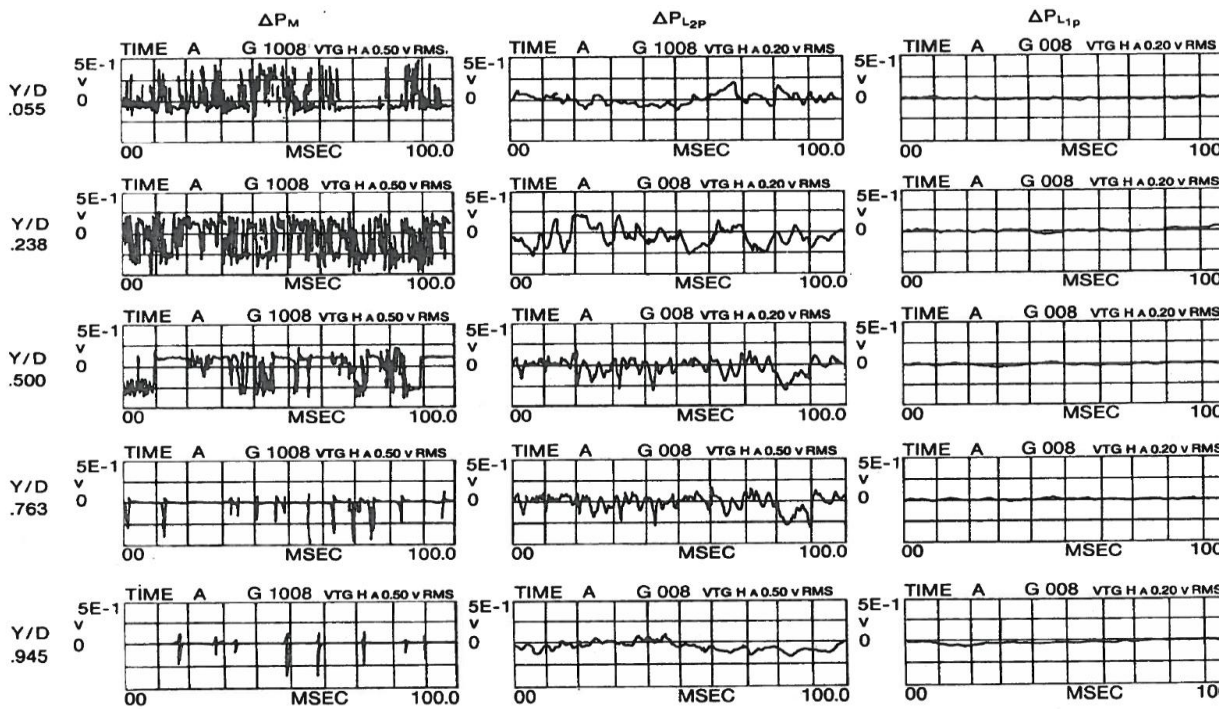
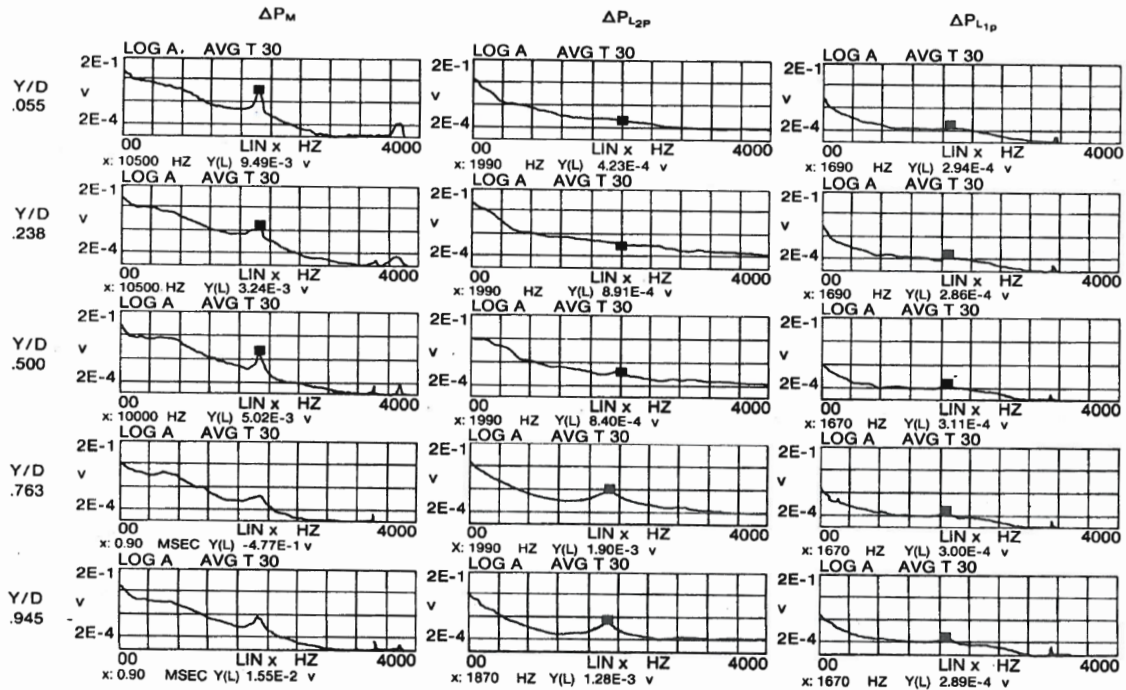


Figure 5: Design of optimum liquid phase isolation.



(a)

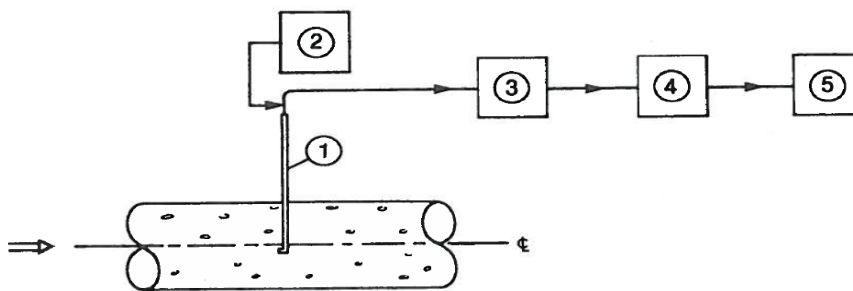


(b)

Figure 6: (a) Typical examples of dynamic pressure signals recorded at axial location 130 D and $X_0 = 0.292$; (b) Broadband frequency spectra of dynamic pressure signals obtained in Figure 7.

Equipment and calibration

The principle of the average dynamic pressure measurement in two-phase flow is illustrated schematically in Figure 7.

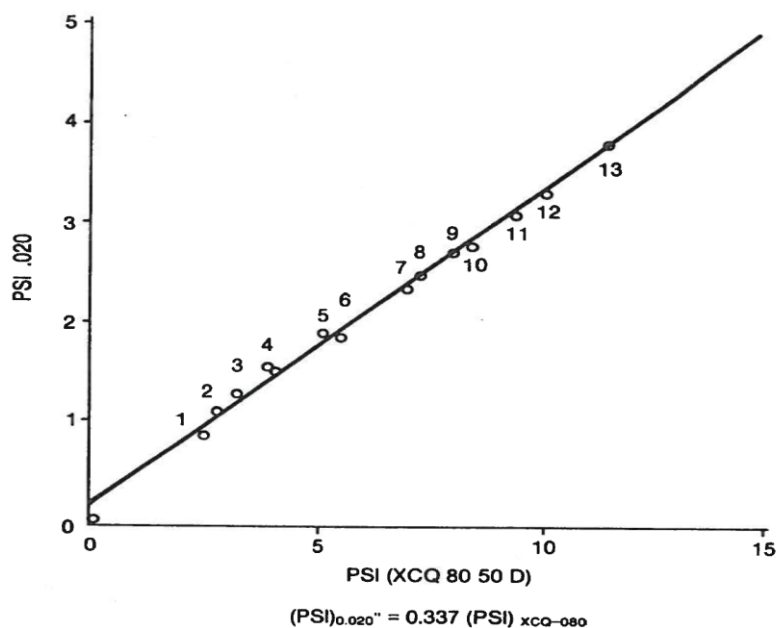


- 1) Miniature pressure transducer (XCQ-080-50D, with or without isolator)
- 2) Power supply (5 V Dc).
- 3) Amplifiers, Filters (ACCUDAIA).
- 4) Oscilloscope (TEKTRONIC).
- 5) Voltmeter (TSI 1076).

Figure 7: Principle and equipment for measurement of the dynamic pressure in two-phase flow.

The calibration curve given in Figure 8 shows a linear relation over the range of water flow rates under consideration. The transducer is placed at the pipe axis and at each specified flow rate the impact pressure is recorded at the output of an integrating digital voltmeter. The same

procedure is repeated with the transducer and liquid isolator system. The measuring period in the latter case is longer and it usually takes about 10 minutes to generate each average value.



USGPM				
1- 2100	4- 2750	7- 3580	10- 3945	13- 4750
2- 2240	5- 3080	8- 3660	11- 4140	
3- 2440	6- 3200	9- 3850	12- 4340	

Figure 8: Calibration curve of a liquid phase isolator in water flow (0.020 in. (0.51 mm) opening width).

The local density of the liquid given at each point is a multiplier of $(1 - \alpha)$, where α is the local void fraction. Since the density of the liquid is the same in single or in two-phase flow under adiabatic conditions, the calibration constant for single-phase flow may be obtained.

The liquid velocity is determined using:

$$U_{L2P} = 11.639 \sqrt{\frac{(\Delta P)d}{\rho_{L2P}L(1 - \alpha)}} \quad (1)$$

where U_{L2P} : liquid phase velocity (ft/sec), ΔP : differential pressure given by the system of transducer XCO-080-50D and liquid isolator 0.020 in (0.51 mm). (psig (kgf/cm²)); d =pipe diameter, L =pipe length, ρ_{L2P} =density and α , the void fraction.

The procedure and equipment for measuring the local void fractions has been previously described by Lakis and Trinh (1988).

EXPERIMENTAL RESULTS

Longitudinal distribution of average velocities in fully developed conditions:

In order to facilitate the observation of flow development along the pipe, measured velocities at the pipe axis, U_{CL} are normalized with the mean velocities deduced from a specified initial flow rate U_0 (superficial or initial flow velocity).

Longitudinal distributions of velocity ratios U_{L1PC}/U_{L0} and U_{MC}/U_{M0} are shown in Figure 9.a and 9.b for single-phase and two-phase flows. (U_{L1PC} and U_{MC} are the liquid velocity and mixture velocity at the pipe axis, respectively).

In single-phase water flow, the normalized velocities tend to increase as the flow moves farther downstream, in accordance with other experiments in which the development of a turbulent boundary layer normally accelerates fluid motion near the pipe axis as long as axial locations $Z/D \approx 100$ (A. Kalpakli, M. Shusser *et al* and R.W. FOX *et al*).

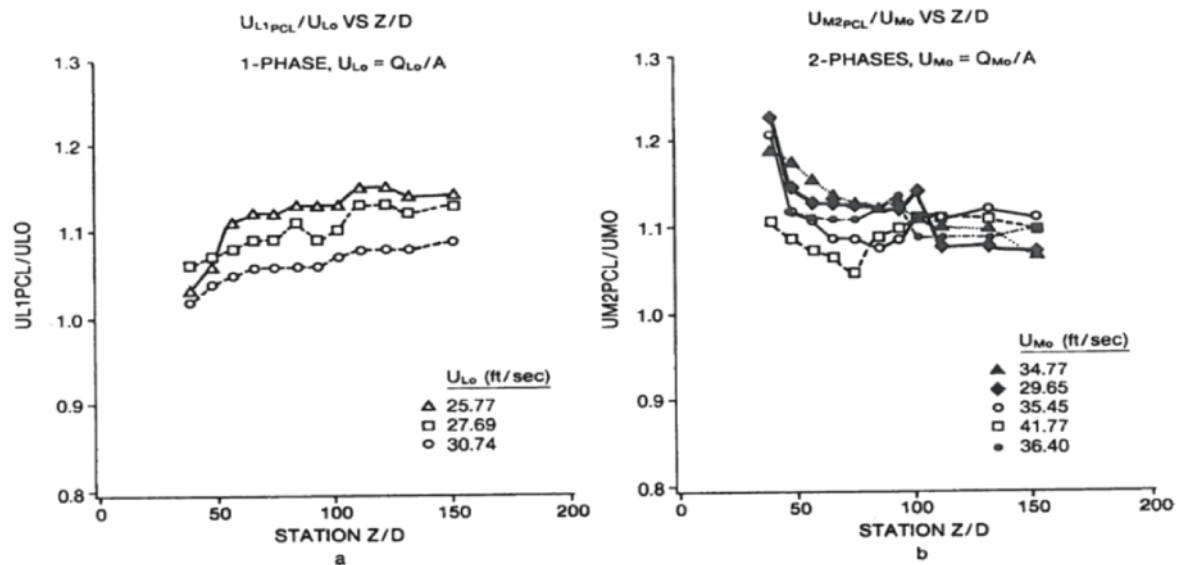


Figure 9: (a) longitudinal variation of velocity ratios (measured values at pipe axis over superficial values) in single-phase flow; (b) Longitudinal variation of velocity ratios (measured values at pipe axis over superficial values) in two-phase flow.

In the presence of air bubbles, the normalized velocities are somewhat arbitrary from one flow volumetric quality to another. However, the violent mixing action almost completely disappears after $Z/D = 110$ as shown in Figure 9.b.

By definition, the flow is supposed to be fully developed when:

- The longitudinal velocity distribution is unchanged. (Single-phase flow).
- The longitudinal void fraction distributions and mixture and phase velocities are statistically unchanged. (Two-phase flow).

The latter can be understood by considering that the forms of the void fraction and the velocity profile remain relatively constant throughout the pipe length.

The variation in liquid velocity profiles measured at three axial downstream locations is given in Figure 10, where measurements were taken at the highest liquid flow rate (≈ 5000 USGPM (≈ 18500 l)) with 11.6 % and 26.4 % as the chosen volumetric qualities.

Examination of velocity ratios in single and two-phase flows (Figures 9.a, 9.b, 10), and of void fraction ratios (Lakis and Trinh, 1988), leads to the following conclusions:

In single-phase water flow, the flow is fully developed at the axial location $Z/D \approx 100$.

In two-phase flow, the flow is fully developed at the axial location $Z/D \geq 100$.

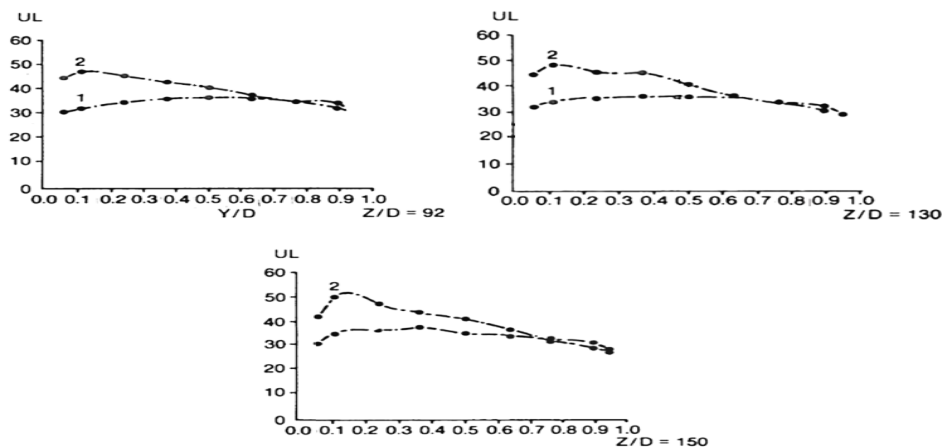


Figure 10: Variation of velocity profiles along three axial locations.
(1: $X_0 = 0.116$, 2: $X_0 = 0.264$, $Q_{L0} = 4373$ USGPM, U_L ft/sec.).

Distribution of continuous phase velocities

In gas-liquid flow with liquid predominating, the initial liquid flow rate U_{L0} plays an important role in producing turbulence and phase separation, and then local flow conditions. Due to the importance of using the same measuring equipment for both single and two-phase flows, we will first present the verification of velocity distribution in single-phase flow.

Validation and comparison

*Average velocity distribution laws for single-phase flow

Measurements of velocity in single-phase water flow may be verified by referring to existing laws that distinguish between the flows in two regions: the core region and the small region close to the pipe wall.

In the core region, a large diameter vortex that is long in the axial direction covers almost all of the pipe cross-section. Small vortices formed within this large one dissipate the energy near the wall. The intensity of the turbulence is almost invariable and it is presumed that the turbulent velocity, for all practical purposes, is constant.

In the region bordering the wall, the flow is influenced by the viscosity of the fluid and nature of the wall.

The principal effect of turbulent energy is related to the pressure drop. Experiments in the past have shown that the ratio of average velocity to friction velocity U/u^* does not depend on pipe radius, and the law of the wall can be applied. In other regions away from the wall, the distribution of the ratio $(U_{CL} - U)/u^*$ no longer depends on the nature of the wall and hardly at all on the viscosity, hence the velocity defect law may be applied.

At a high Reynolds number, experiments have also indicated that there is a “recovery zone” where the two laws mentioned above apply simultaneously. In this zone, the velocity distribution obeys a logarithmic or universal law.

***Power law**

The determination of velocity distribution in turbulent flow is usually based both on logical hypothesis and experimental verification. In fully developed turbulent flow, the time-averaged velocity is invariant with vertical position. The independent variables that are supposed to affect the velocity are: fluid density, dynamic viscosity of the fluid, pipe diameter, vertical position, pipe wall roughness and average wall shear stress. Water flow experiments by Nikuradse *et al.* have demonstrated that the velocity profile may be approximated by a power law.

Results of experiments carried out in this study agree very well with those of Nikuradse. The final results of regression analysis are:

$$\frac{U}{U_{CL}} = (1 - |2y^* - 1|)^{0.091} \quad (2)$$

($Re = 2 \times 10^6$, arithmetic mean deviation = -1.3 %, standard deviation = 0.2 %). Where U : time-averaged local liquid velocity, U_{CL} : liquid velocity at pipe axis and y^* : y/D , normalized vertical position measured from the pipe wall.

Velocity defect law

The effect of viscosity on flow is noticeable only in the region near the wall, where the velocity gradient is much greater than that near the pipe axis. The wall roughness, which affects the friction velocity u^* for a given flow rate, has a slight influence on the flow near the pipe axis. It may be presumed that the difference $U_{max} - U$ depends uniquely on vertical position according to the following relation:

$$\frac{U_{max} - U}{u^*} = A_1 \log_{10} \left(\frac{R}{y} \right) \quad (3)$$

where U_{max} : maximum velocity attained at pipe axis = U_C , U : local liquid velocity, u^* : friction velocity ($= \sqrt{\tau_n / l_L}$), R : pipe radius, Y : distance measured from pipe wall and A_1 : unknown constant.

The wall shear stress is determined either by measured pressure drop or by existing friction coefficient correlations (This correlation is valid for void fraction in a range of $0 \leq a \leq 0.5$). Our experimental results yield:

$$\frac{U_{CL} - U}{u^*} = 4.85 \log_{10} \left(\frac{1}{1 - |2y^* - 1|} \right) \quad (4)$$

($Re = 2 \times 10^6$, arithmetic mean deviation = 19.4 %, standard deviation = 4 %).

*** Universal distribution of velocities** (in the neighborhood of the smooth wall, high Re)

At very high Reynolds numbers, the velocity of the mixture near the wall is independent of pipe radius and the mean velocity at the same vertical position depends only on τ_w , ρ and μ . Under these conditions the experimental results show that the distribution of the velocity may be predicted by a "logarithmic profile":

$$\frac{U}{u^*} = A \ln \eta + B \quad (5)$$

where :

$$\eta = \frac{1 - |2y^* - 1| Ru^*}{\nu} \quad (6)$$

ν : Kinematic viscosity of the fluid, u^* : friction velocity ($=(\tau_w / \rho)^{1/2}$), U : local velocity, and R : pipe radius. A and B are determined by linear regression and Equation (5) becomes:

$$\frac{U}{u^*} = 2.07 \ln \eta + 6.42 \quad (7)$$

(Arithmetic mean deviation = -5.8 %, standard deviation = 0.2 %)

*Other considerations

By integrating Equation (4) over the pipe cross-section, the average velocity flow is obtained:

$$\bar{U} = U_C - au^* \quad (8)$$

Where: \bar{U} : average velocity in the cross-section, U_{CL} : measured velocity at the centerline of the pipe, u^* : friction velocity and a : unknown constant.

The constant “ a ” is determined empirically, giving the following result:

$$\bar{U} = U_C - 3.82 u^* \quad (9)$$

(Arithmetic mean deviation = 1.4 % standard deviation = 7.6 %).

Rewriting (4) in the form:

$$\frac{U_{CL}}{u^*} = \frac{U}{u^*} + 2.11 \ln (1 - |2y^* - 1|) \quad (10)$$

we obtain, by substituting U_{CL} / u^* into Equation (7):

$$\frac{U_{CL}}{u^*} = 2.11 \ln \left(\frac{Ru^*}{\nu} \right) + 6.42 \quad (11)$$

and by substituting (11) into (9):

$$\frac{U}{u^*} = 2.11 \ln \left(\frac{Ru^*}{\nu} \right) + 2.60 \quad (12)$$

A comparison of the principal laws (Equations (2), (4) and (7)) with the literature (Schlichting *et al.*) is presented in Figure 11.

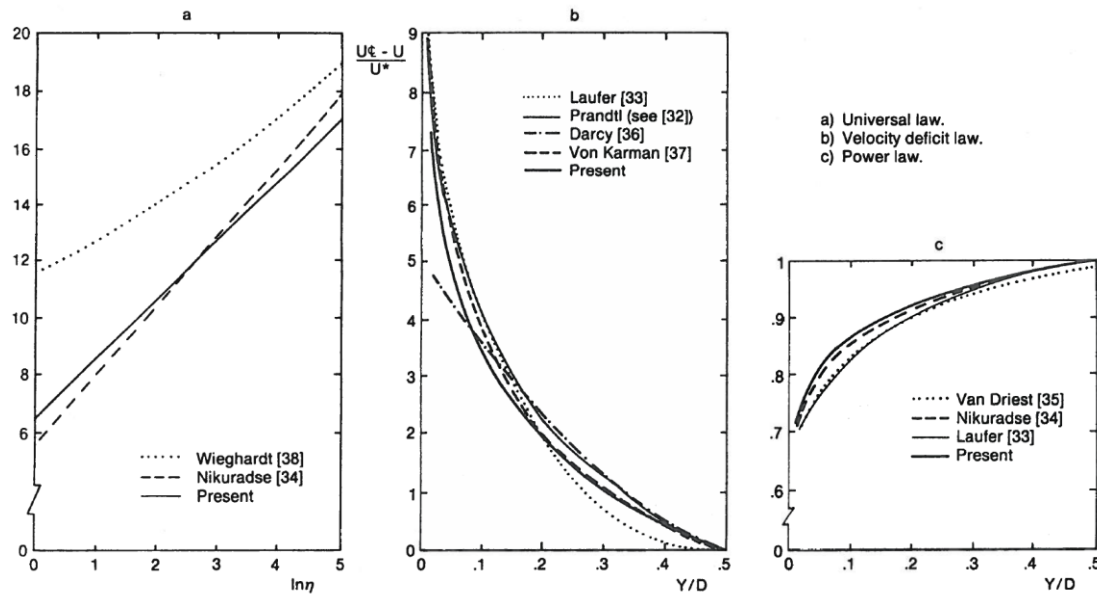


Figure 11: Verification of average velocity distribution laws in single-phase flow.

Cross-sectional distribution of liquid velocities in two-phase gas-liquid flow

a- Transverse plane

Assuming that the flow is stationary and ergodic, substitution of the average values of the differential pressure ΔP and the void fraction α at a vertical position, y/D into Equation (1) gives the average velocity of this phase; U_{L2P} . Liquid phase velocity profiles in the transverse plane are shown in Figure 12.a. The profiles of normalized velocity, U_{L2P} / U_{L2PC} with a different flow volumetric quality,

$X_0 = 0.219$, and for a range of stations, z/D are shown in Figure 13.a. and 13.b, U_{L2PC} is the average velocity of the liquid phase measured at the pipe axis for a given z/D over a range of X_0 . The profiles are essentially uniform at the beginning and become increasingly asymmetrical as z/D increases.

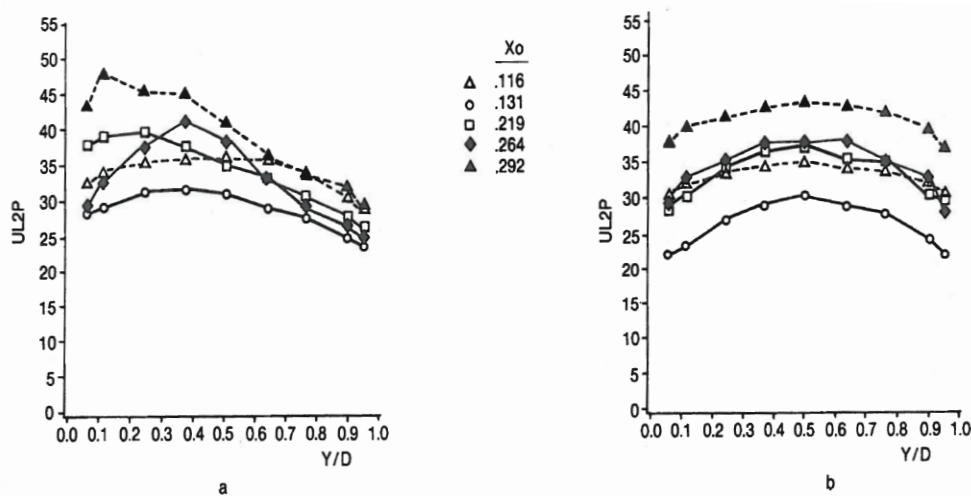


Figure 12: (a) Distribution of liquid phase velocity in horizontal plane; (b) Distribution of liquid phase velocity in vertical plane.

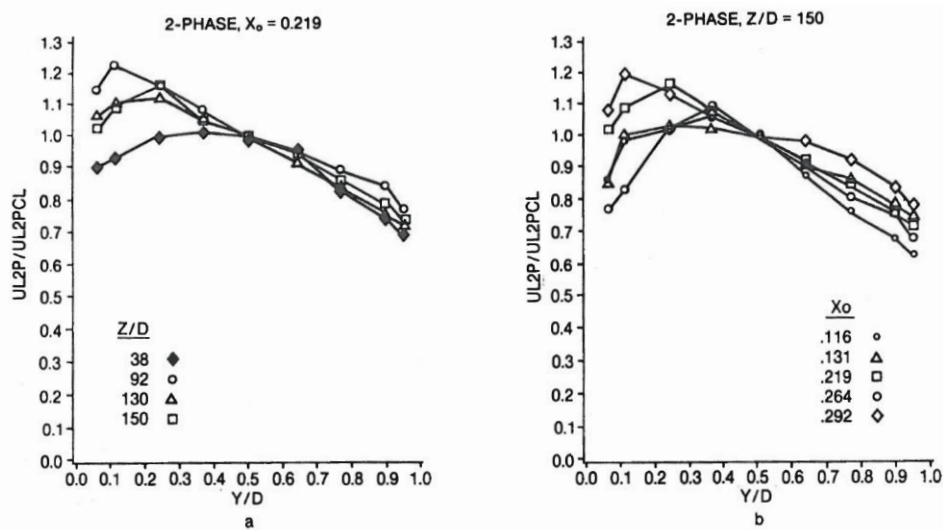


Figure 13: (a) Vertical distribution of ratio U_L/U_{LC} at $X_0 = 0.219$ and various axial locations; (b) Vertical distribution of ratio U_L/U_{LC} at 150 D axial location and various flow volumetric qualities.

The asymmetry remains unchanged, even while the separation of the phases is in equilibrium with the diffusion rate in the entrained phase.

For a constant water flow rate, any increase in the injected airflow rate leads to an acceleration of the liquid phase in the upper half of the pipe, especially in the passages containing a strong concentration of void fraction. This displacement effect of the injected air on the flowing water is, however, much weaker in the lower half of the pipe, particularly near the bottom. The velocity of the liquid phase in this region is smaller than that for single-phase when the airflow rate is sufficiently low, and the two are nearly equal at high injected airflow rates.

As the air flow rate increases, acceleration is generally more significant in the upper part of the pipe. Ohba *et al.* also made this observation in their study of a vertically ascending flow; the concentration of bubbles is greater at the periphery of the pipe as airflow rate increases.

At a constant airflow rate, an increase in water flow rate always accelerates the liquid phase. For low water flow rates, the profiles measured upstream of $z/D = 90$ may be calculated (or evaluated) using a power law. Beyond this distance, the profile form resembles that of the void fraction.

b- Vertical plane

Liquid phase velocity distribution in the vertical plane is uniform throughout the pipe cross-section, as illustrated in Figure 12.b.

In this plane, separation of the phases by gravity has no influence on the velocity distribution profiles. Only turbulent diffusion of the entrained phase affects the homogeneity of the liquid phase velocity distribution. The void fraction profile is therefore uniform, which leads to a uniform liquid phase velocity.

Although the void fraction has a tendency to disperse towards the wall when the air flow rate increases, the difference between values near the wall and those near the pipe axis is not significant, and the acceleration of the bubbles has no effect on the liquid velocity near the pipe axis (Morgan *et al.* 2013).

If the void fraction distribution α is nearly constant, the liquid velocity increases as in single-phase flow. The distribution form may be approximated using a power law as in the case of vertical flow (Serizawa *et al.*, Ohba *et al.*).

If the characteristics of the profile (U / U_{CL} for example) are compared with those of single-phase flow, the difference is very small, which agrees well with the results of Burdukov and Valukina, ($Re = 13400$), who used the electrochemical method to determine the velocities and found the exponent to be between 1/6 and 1/7 (Figure 14).

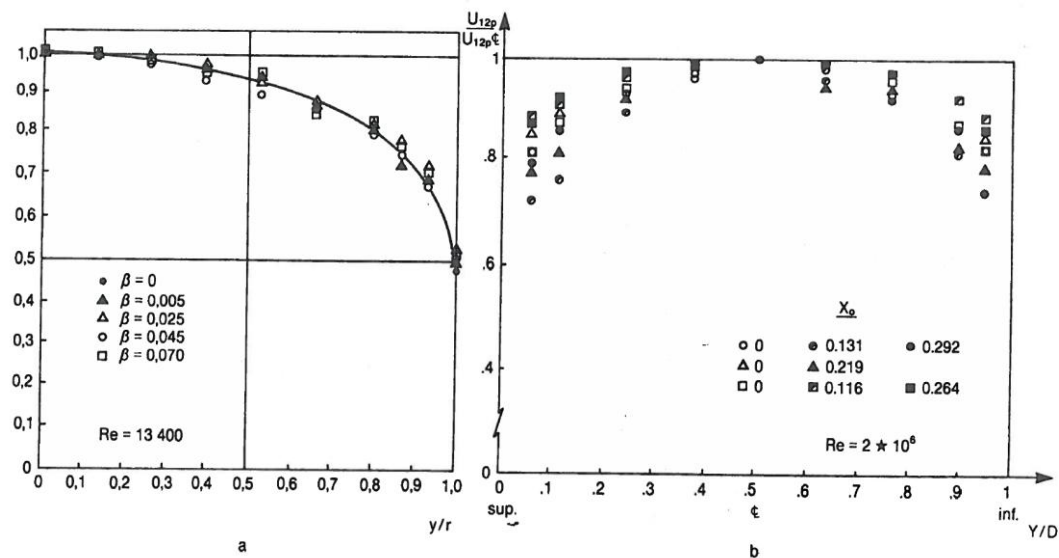


Figure 14: Vertical distribution of liquid phase velocity in small diameter pipe (5) and large diameter pipe (present, 8.6-in. (218.44 mm)).

RESULTS AND PROPOSED CORRELATIONS

Proposed correlation

According to our observations, liquid phase velocity profiles may be approximated using a power law, an approach that has been employed by several researchers. The analysis of velocity profiles in the proceeding section permits deduction of the relationship:

$U_{L2P} = f(X_0, \alpha)$, in which the void fraction, α is a function of the flow volumetric quality, X_0 and the vertical position y/D .

However, approximation using the power law does not seem valid except in the vertical plane where profile symmetry exists. In addition, prediction of the liquid phase velocity of a predominantly liquid flow may be more direct and easier to achieve if the liquid velocity of a single-phase flow is considered as an explicit variable in the relation.

To verify this hypothesis, the ratio between the local liquid velocities of two-phase and single-phase flow is expressed in terms of the void fraction as illustrated in Figure 15. We

note the existence of a linear dependence between the ratio of velocities U_{L2P}/U_{L1P} and the void fraction α .

Linear regression generates the following relation:

$$\frac{U_{L2P}}{U_{L1P}} = 1 + 0.842 \alpha \quad (13)$$

This relation is valid for all values of α , $0 \leq \alpha \leq 0.5$. Values calculated using this relation are compared with experimental results in Figure 16 (arithmetic deviation = 1.2 %, standard deviation = 1.1 %).

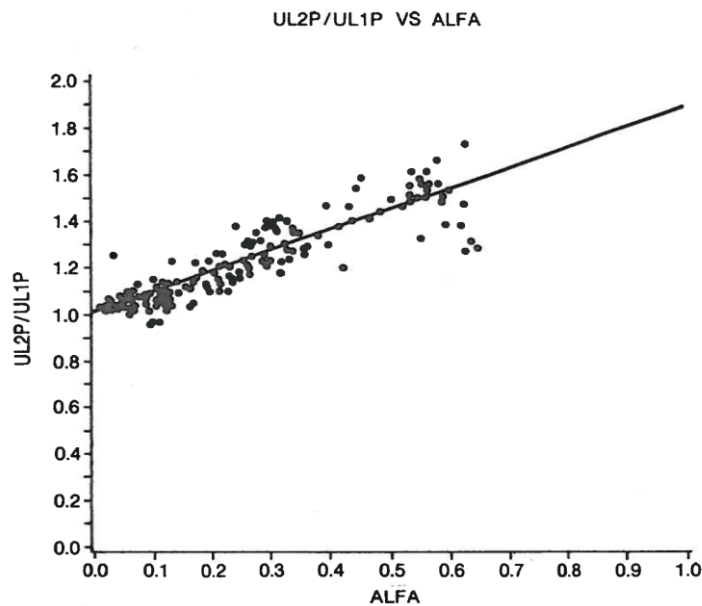


Figure 15: Variation of ratios $UL2P/UL1P$ in terms of void fraction.

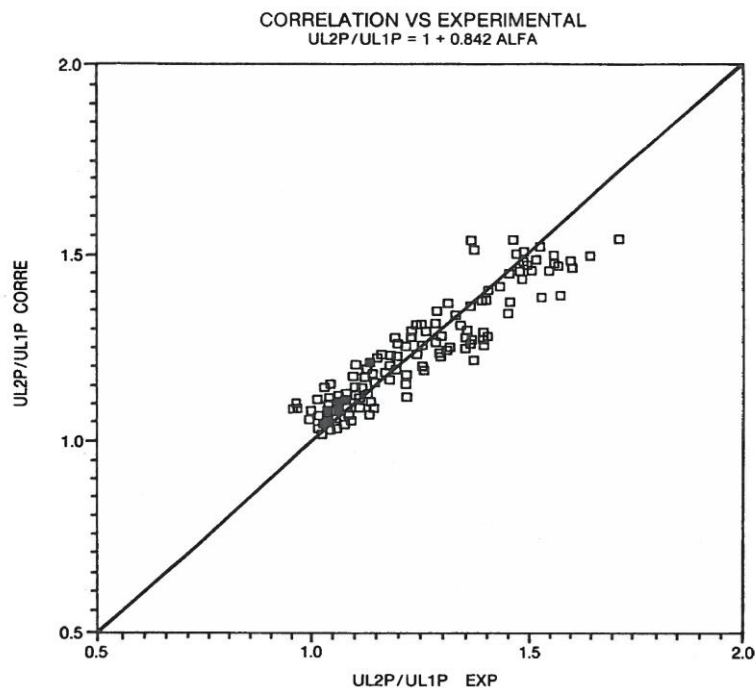


Figure 16: Comparison between values estimated by the proposed relation and experimental results.

Numerical Analysis

A force balance applied to an element in the liquid phase of a statistically steady flow yields the equations of motion of this phase. The vertical gradient of velocity in the liquid phase is related to the eddy diffusivity of the liquid and the interaction stress between the two phases (Lari, K., *et al.*, 2010).

The profile of the shear stress τ_{int} is obtained by calculating a numerical integral over the pipe diameter. Furthermore, in cases where the static pressure gradient is constant, a simplified expression is obtained for a fully-developed flow.

According to Sato and Seroguchi, the shear stress of the liquid phase can be separated into two parts, one corresponding to components of velocity due to the inherent turbulence of the liquid only, and the other two velocity components generated by the supplementary turbulence of liquid caused by agitation of the bubbles.

Equations of motion for two-phase dispersed bubbles flow

The governing equations for unsteady two-phase dispersed flow are given by Equations (14) and (18) in a study by Lakis, A. A., and Trinh, N. D. (1988).

If the flow is statistically steady, the time-averaged acceleration of the fluid equals zero and the forces acting on an element of fluid must be in balance. We then obtain Equations (19) and (20), again referring to the above study. Further, using Equations (26) and (27) of the same reference, the liquid phase velocity becomes:

$$\frac{d\phi_L}{dr^*} = \left[-\frac{1}{r^*} \frac{r^{*2} - 2 \int_0^{r^*} \alpha r^* dr^*}{1 - 2 \int_0^{r^*} \alpha r^* dr^*} + \frac{R}{L_r^*} \frac{d}{dz^*} \left(\int_0^{r^*} P_L^* r^* dr^* - \int_0^{r^*} P_L^* r^* dr^* \frac{r^{*2} - 2 \int_0^{r^*} \alpha r^* dr^*}{1 - 2 \int_0^{r^*} \alpha r^* dr^*} \right) \right] \quad (14)$$

where U_{2p}^* is the friction velocity in two-phase flow,

$$r^* = \frac{r}{R},$$

$$Z^* = Z/L,$$

ϕ_L is the non-dimensional velocity of liquid ($\phi_0 = U_L / U_{2p}^*$),

$$\varepsilon_{2p}^* = \varepsilon_{2p} / R U_{2p}^* \quad (15)$$

$$P_L^* = \frac{(1-\alpha)P_m}{P_L U_{2p}^*} \quad (16)$$

$$U_{2p}^* = (\tau_{w2p} / P_L)^{1/2} \quad (17)$$

α is the local void fraction,

ε_{2p} is the eddy diffusivity of the two-phase flow,

τ_{w2p} is the wall shear stress,

P_L is the density of fluid,

P_M is the static pressure of the mixture flow.

If the flow is fully developed, all fluid variables (velocity, pressure, void fraction, etc.) remain constant in the direction of the flow. This proposition implies that, from Equation (27):

$$\frac{d}{dz^*} [\dots\dots\dots] = 0 \tag{18}$$

we then have:

$$\frac{d\phi_L}{dr^*} = \frac{1}{\varepsilon_{2p}^*} \left[-\frac{1}{r^*} \cdot \frac{r^{*2} - 2 \int_0^{r^*} \alpha r^* dr^*}{1 - 2 \int_0^{r^*} \alpha r^* dr^*} \right] \tag{19}$$

Rewriting Equation (19) by replacing the eddy diffusivity in two-phase flow (ε_{2p}^*) by the value given in reference Sato, Y., *et al.*, (1975), we obtain:

$$d\phi_L = \frac{1}{b(1-\alpha)} \cdot \frac{a_i - r^{*2}}{r^* (-0.1790r^{*4} + 0.1192r^{*2} + f_i)} dr^* \tag{20}$$

where:

$$\varepsilon_{2p}^* = (1-\alpha)(-0.18r^{*4} + 0.12r^{*2} + f_i) \tag{21}$$

$$f_i = \frac{\nu_L}{Ru_{2p}^*} + \frac{K'' \bar{r}_G \bar{U}_G \alpha}{Ru_{2p}^*} + 0.06 \tag{22}$$

$$U_{2p}^* = (\tau_{w2p} / P_L)^{1/2} \tag{23}$$

K'' is an unknown constant,

\bar{r}_G is the mean local velocity of bubbles (space average),

ν_L is the kinematic viscosity of liquid,

α is the void fraction.

Also,

$$a_i = 2 \int_0^{r^*} \alpha r^* dr^* \qquad b = 1 - 2 \int_0^1 \alpha r^* dr^*$$

According to the step-like arrangement shown in Figure 17.b, integration of Equation (12) in the new coordinates allows us to obtain:

$$r^* = | 2y^* - 1 | \tag{24}$$

where: $y^* = \frac{y}{D}$

$$\int_{\phi_{i-1}}^{\phi_i} d\phi_L = \frac{1}{b(1-\alpha)} \left[\int_{r_i^*}^{r_{i+1}^*} \frac{a_i dr^*}{r^* (Ar^{*4} + Br^{*2} + C_i)} - \int_{r_i^*}^{r_{i+1}^*} \frac{r^* dr^*}{Ar^{*4} + Br^{*2} + C_i} \right] \tag{25}$$

where: $A = -0.18$, $B = 0.12$, $C_i = f_i$.

We then obtain for fully-developed flow:

$$\phi_{L_i} = \phi_{L_{i+1}} + \frac{1}{1-\alpha_i} \frac{a_i}{4bC_i F_i} \left[F_i (H_{i+1} - H_i) - (G_{i+1} - G_i) \left(\frac{2C_i}{a_i} + 0.1192 \right) \right] \tag{26}$$

where: $i = 1, 2, \dots, n-1$

n : number of points (= number of vertical positions in the half channel (including the centerline position) +1)

$$C_i = \frac{v_L}{Ru^*_{2p}} + \frac{K'' \bar{r}_G \bar{U}_A \alpha_i}{Ru^*_{2p}} + 0.06 \tag{27}$$

$$F_i = (0.0142 + 0.7160C_i)0.5 \tag{28}$$

$$G_{(i)(i+1)} = \ln \left| \frac{-0.3580 |2y^{*(i)(i+1)} - 1|^2 + 0.1192 - F_i}{-0.3580 |2y^{*(i)(i+1)} - 1|^2 + 0.1192 + F_i} \right| \tag{29}$$

$$H_{(i)(i+1)} = \ln \left| \frac{|2y^{*(i)(i+1)} - 1|^4}{-0.1790 |2y^{*(i)(i+1)} - 1|^4 + 0.1192 |2y^{*(i)(i+1)} - 1|^2 + C_i} \right| \tag{30}$$

$$\phi_L = \frac{U_L}{u^*_{2p}}$$

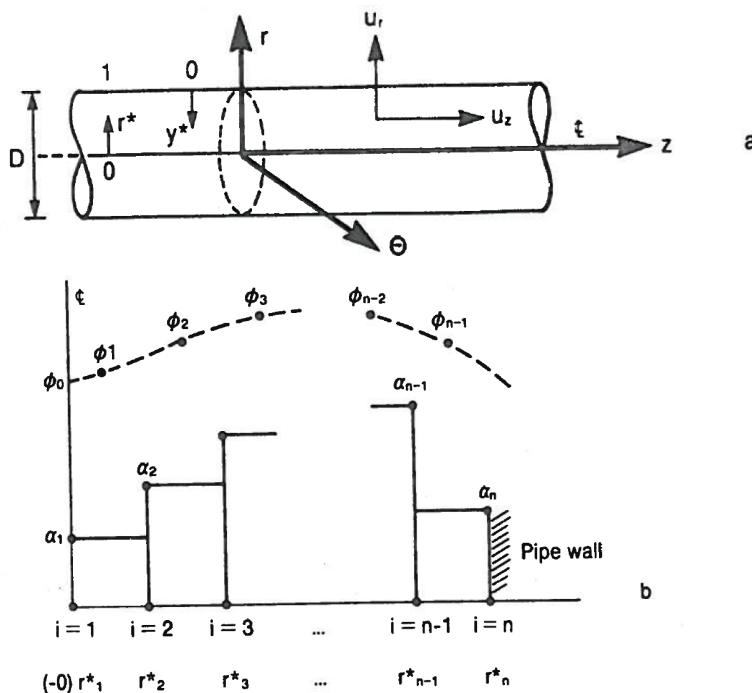


Figure 17: (a) Pipe coordinates; (b) Step-like arrangement for numerical computation of liquid velocity and void fraction.

Distribution of liquid velocity in single-phase flow

If $\alpha_i = 0$, we have, according to Equation (27),

$$\phi_{L1P_i} = \phi_{L1P_{i+1}} + \frac{1}{2F_i} (G_i - G_{i+1}) \quad (31)$$

with $\phi_L = \frac{U_{L1P}}{U_{1P}^*}$, and

$$C_i = \frac{v_L}{Ru_{1P}^*} + 0.06 \quad (32)$$

A comparison of numerical model and experimental results is given in Figures (18a and 18b) and (19) for velocity and shear stress distributions in two-phase flow, respectively.

The graphs indicate that the numerical model offers better results in the vertical plane than in the transversal plane.

In the transversal plane, numerical results are still comparable at low airflow rates. Discrepancies start to appear when the volumetric quality flow $X_0 \geq 20\%$. In order to obtain better results in the transversal plane we suggest that future formulations be based on two-dimensional analysis of the flow and that lift, drag, and mass forces be taken into account. The normalized Root-Mean Square Deviation (NRMSD) has been calculated (see Fig 18a and 18b). We may conclude that in the transversal planes and in the vertical planes the numerical results are practically similar to those of experimental in the range between 80 and 100%.

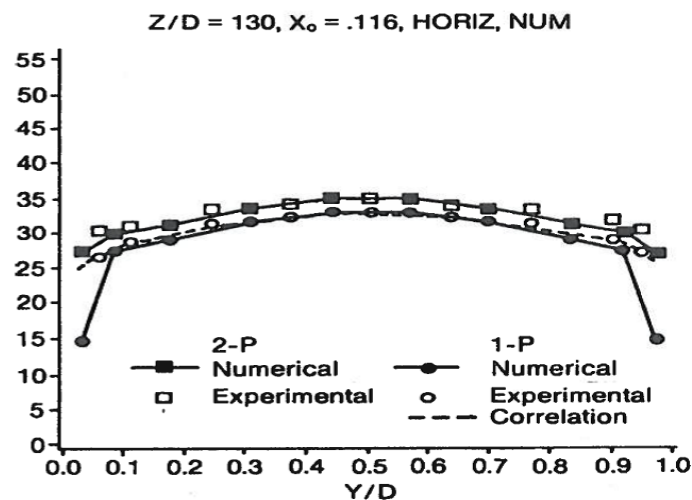


Figure 18: a) Numerical results of liquid phase velocity profiles: **transversal plane**.

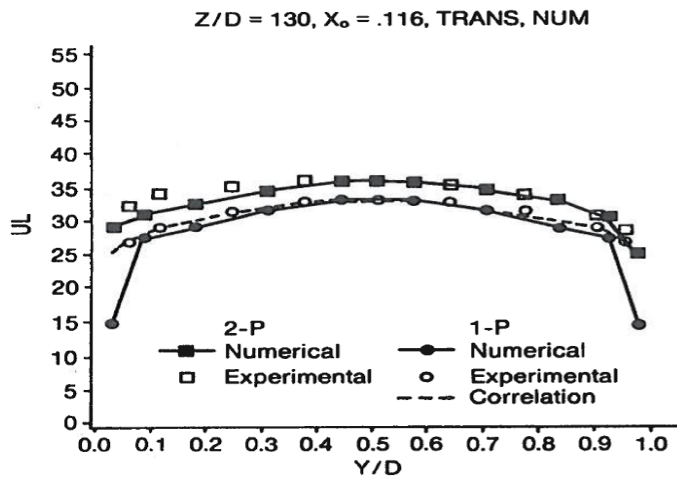


Figure 18: b) Numerical results of liquid phase velocity profiles: **Horizontal plane.**

Normalized Root-Mean Square Deviation (NRMSD):

<u>Numerical</u> 1-P Curves		<u>Experimental</u> 1-P Curves		<u>Numerical</u> 2-P Curves		<u>Experimental</u> 2-P Curves	
X	Y	X	Y	X	Y	X	Y
0.29	21.9	0.28	21.8	0.29	23.4	0.28	23.9
0.35	22.6	0.31	22.5	0.35	24.2	0.31	24.9
0.44	23.7	0.40	23.6	0.44	24.9	0.40	25.2
0.52	24.4	0.49	24.2	0.53	25.6	0.53	25.6
0.61	24.3	0.57	24.3	0.57	25.7	0.57	25.7
0.70	23.6	0.66	24.1	0.62	25.6	0.62	25.6
0.79	22.3	0.75	23.6	0.66	25.4	0.70	25.1
0.85	21.7	0.84	22.5	0.70	25.1	0.75	24.7
				0.75	24.8	0.79	24.3
				0.79	24.4	0.83	23.3
				0.83	23.4	0.85	22.7

NRMSD=2.3

NRMSD=2.0

Normalized Root-Mean Square Deviation (NRMSD):

Numerical		Experimental		Numerical		Experimental	
1-P Curves		1-P Curves		2-P Curves		2-P Curves	
X	Y	X	Y	X	Y	X	Y
1.25	21.9	1.27	22.5	1.25	23.1	1.25	23.3
1.31	22.7	1.36	23.7	1.31	23.8	1.36	24.8
1.40	23.8	1.40	23.9	1.39	24.8	1.39	24.9
1.49	24.4	1.49	24.5	1.48	25.5	1.49	25.4
1.57	24.5	1.57	24.5	1.57	25.5	1.57	25.5
1.65	23.8	1.66	23.9	1.66	24.9	1.65	24.8
1.75	22.8	1.70	23.6	1.75	23.9	1.71	24.5
1.80	22.0	1.79	22.5	1.80	23.3	1.79	23.9
NRMSD=2.1				NRMSD=1.9			

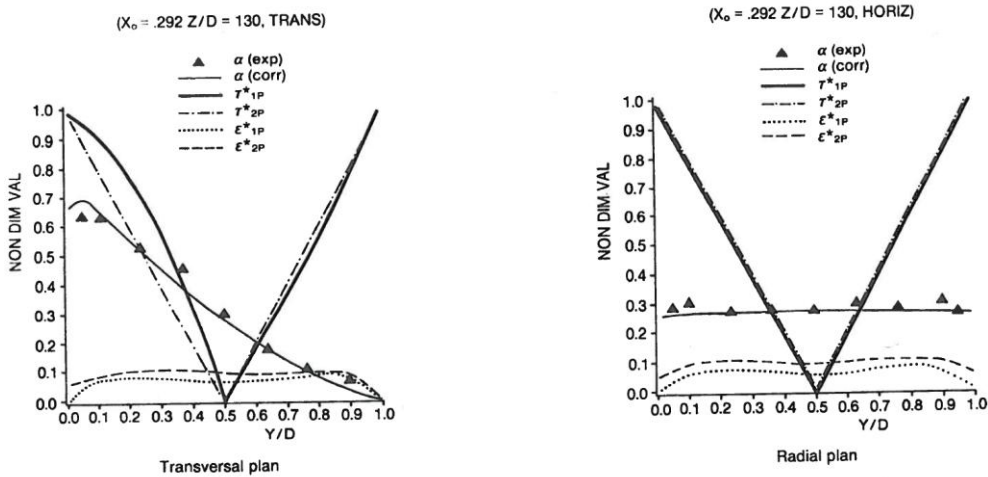


Figure 19: Numerical results of shear stress distribution in dispersed bubble flow.

CONCLUSION

One way to determine the local liquid-phase velocity is through use of a liquid isolator (or bubble eliminator) with a miniature pressure transducer or a Pitot tube to facilitate measurement and interpretation of impact pressure in two-phase flow. Its design takes into consideration minimum perturbation at local measuring points and provides maximum efficiency in eliminating bubbles along with a reasonable measuring period. Liquid phase velocity can then be deduced provided that local liquid density is known. The reliability of this indirect method depends on the calibration procedure.

Experimental results indicate that the velocity profiles resemble those of single-phase flow for various chosen values of flow volumetric quality in a vertical plane.

It was also observed that the form of the velocity profiles is similar for both small and large diameter pipes.

In the transversal plane, asymmetry of the profiles appears from $X \geq 12\%$ and remains unchanged for axial locations in the range $z/D \geq 100$, where the two-phase flow is assumed to be completely developed.

The velocity of the continuous phase (liquid) and the void fraction strongly influence phase distribution in the pipe. The ratio of velocity in two-phase flow to that in single-phase flow was found to be a linear function of the void fraction in the range of $0 \leq a \leq 0.5$.

Based on the assumption of turbulent shear stress in bubble flow given by Sato and Seroguchi *et al* (1975), a numerical model was developed to predict the distribution of liquid velocity and shear stress in dispersed bubble flow. The numerical model includes the eddy diffusivity relationship in single-phase water flow proposed by Travis *et al.*, the measured values of pressure drop, the mean local velocity of the bubbles, the mean bubble diameter and the local void fraction in fully-developed flow.

Numerical results agree well with measurements in the vertical plane. Discrepancies between numerical and experimental results in the transversal plane were noted at flow volumetric quality values $X_0 \geq 20\%$. Lift, drag and mass forces seem to be important in horizontal flow and we suggest that these be included in future numerical analysis studies.

REFERENCES

1. ALIA, P., CRAVAROLO, L., HASSID, A., PETROCCHI, E. (1968), "Phase and Velocity Distribution in Two-Phase Adiabatic Annular Dispersed Flow", *Energies Nuclear*, vol. 15, no. 4, April 1968, p. 242-254.
2. ANDERSON, G. H., MANTZOURANIS, B. G. (1960), "Two Phase (Gas-Liquid) Flow Phenomena II. Liquid Entrainment". *Chemical Engineering Science*, vol. 12, no. 4, p. 233-242.
3. BANKOFF, S.G. (1960), "A Variable Density Single Fluid Model for Two-Phase Flow with Particular Reference to Steam-Water Flow", *J. of Heat Transfer, Trans. ASME*, ser. C., vol. 82, Nov., p. 265-272.
4. BROWN, F. C. KRANICH, W. L. (1968), "A model for the prediction of velocity and void fraction profiles in two-phase flow", *AICHE*, vol. 14, Sept., p. 750-758.
5. BROWN, R. W., GOMEZPLATA, A., PRICE, J. D. (1969), "A Model to Predict Void Fraction in Two-Phase Flow", *Chemical Engineering Science*, vol. 24, p. 1483-1489.

6. BURDUKOV, A. P., VALUKINA, N. V. (1975), "Special Characteristics of the Flow of a Gas-Liquid Bubble Type Mixture with Small Reynolds Numbers", *Shurnal Prik. Mekh. Tech. Fiziki*, no. 4, p. 137-141.
7. CHEN, K.S. YANG, Y. J. CHANG, and WANG C.C. "Two-phase pressure drop of air-water and R-410A in small horizontal tubes". *Int. J. Multiphase Flow*, 27 (2001), pp. 1293-1299.
8. DELHAYE, J. M. (1969), "Hot Film Anemometry in Two-Phase Flow", *Proc. 11th Nat. ASME/AICHE Heat Transfer Conf. On two-phase Instr.*, Minneapolis (Minnesota), p. 58-69.
9. SERIZAWA, A., KATAOKA, I., MICHİYOSHI, I. (1975), "Turbulent Structure of Air-Water Bubbly Flow I. Measuring Techniques", *Int. J. Multiphase flow*, vol. 2, p. 221-233.
10. FINCKE, J. R., DEASON, V. A. (1978), "Fluid Dynamics Measurements in Air-Water Mixtures Using a Pitot tube and Gamma Densitometer". *ISA, ISDN 87664 407 8*, p. 621-626.
11. GALAUP, J. P. (1975), "Contribution à l'étude des méthodes de mesure en écoulement diphasique", *Thèse de Doctorat, Université de Grenoble*.
12. GILL, L. E., HEWITT, G. F., HITCHEN, J. W. (1962), "Sampling Probe Studies of the Gas Core in Annular Two-Phase flow. Part 1. The Effect of Length on Phase Velocity Distribution", *AERE R*, no. 3954.
13. GORIN, A. V. (1978), "Friction and the Velocity and Gas Content Profiles of a Turbulent Gas-Liquid Flow", *J. of Engineering Physics*, vol. 35, Sept., no. 3, p. 1029-1036.
14. HALBRONN, G. (1951), "Mesure des concentrations et des vitesses dans un courant mixte d'air et d'eau". *La Houille Blanche*, Mai-Juin, p. 394.
15. JEPSEN, J. C., RALPH, J. L., (1970), "Hydrodynamic studies of Two-Phase Up flow in Vertical Pipelines". *Proc. Instn. Mech. Engrs.*, (1969-70), vol. 184, Part 3C. Communication 20, p. 154-165.
16. KASHINSKY, O. N., RANDIN, V. V.; TIMKIN, L. S. (1994), "Direction-specific characteristics of a three-component electrodiffusional Velocity probe", *Journal of Applied Electrochemistry*, vol. 24, July, p. 694-696.
17. KINOSHITA, T., MURASAKI, T. (1969), "On a Stochastic Approach to the Pulsating Phenomena in the Two-Phase Flow". *ISME*, vol. 12, no. 52, p. 819-826.
18. KOZMIENKO, B. K., NAKORIAKOW, W. E., BURDUKOW, A. P., KOWALSKI, J., SLIWICKI, E. (1976), "Velocity Profile of the Liquid Phase in a Two-Phase Flow with Bubble Structure". (in Polish). *Polska Akademia Nauk, Prace Instytutu Maszyn Przeplywowych*, p. 23-29.
19. KRASCHEEV, V. M., MURANOV, YU. V. (1968), "Calculation of Velocity Profile in Two-Phase Dispersed Annular Flow", *High Temperature*, vol. 14, Set. Oct., no. 5, p. 901- 907.
20. LAKIS, A. A., MOHAMED, S. S. (1979), "Pitot Tube Measurements in Fully Developed Turbulent Dispersed Flow". *Multiphase Transport, Fundamentals, Reactor Safety, Application. Eq. N. Veziroviu*, vol. 5, April, p. 2605-2619.
21. LAKIS, A. A., TRINH, N. D. (1988), "Void Fraction in Highly Turbulent and Large Diameter Horizontal Pipe Flow". Report no. EPM/RT 88-24, *École Polytechnique de Montréal. Québec, Canada*.
22. LAKIS, A. A. (1978), "Numerical Analysis of Wall Pressure Fluctuations in Two-Phase Flow", *Numerical methods in laminar and turbulent flow, 17th 21st, Proc. of 5th Int. Cont., Univ. Coll. Swansea, UK*, p. 757-767.
23. LARI, K., VAN Reeuwijk, M., and MAKSIMOVIC, Č. (2010). "Simplified Numerical and Analytical Approach for Solutes in Turbulent Flow Reacting with Smooth Pipe Walls." *J. Hydraul. Eng.*, 136(9), 626-632.
24. LEVY, S. (1963), "Prediction of Two-Phase Pressure Drop and Density Distribution from Mixing Length Theory", *J. of Heat Transfer, Trans. ASME, ser. C.*, vol. 85, May, p. 137-152.

25. MINEMURA, K. UCHIYAMA, T. (1993), "Three-dimensional calculation of air-water two-phase flow in centrifugal pump impeller based on a bubbly flow model", *Journal of Fluids Engineering*, vol. 115, Dec., p. 766-771.
26. MITCHELL, J., HANRATTY, T. J. (1966), "A Study of Turbulent at a Wall Using an Electrochemical Wall Shear Stress Meter", *J. Fluid Mech.*, vol. 26, p. 199-221.
27. NAKORYAKOV, V. E; KASHINSKY, O. N; Randin, V. V (1996), "Gas-liquid bubbly flow in vertical pipes", *Journal of Fluids Engineering*, vol. 118, June, p. 377-382.
28. NIKURADSE, J. (1932), "GesetzmaBigheit der Turbulenten Stromung in Glatten Rohren, *Forsch. Arb. Ing*", WES no. 356.
29. OHBA, K., KISHIMOTO, I., OGASAWARA, M. (1977), "Simultaneous Measurement of Local Liquid Velocity and Void Fraction in Bubbly Flows Using a Gas Laser Part II. Local Properties of Turbulent Bubbly Flow". *Technol. Rep. Osaka Univ.*, vol. 27, Mars, no. 1358, p. 228-238.
30. PANNEK, S.; PAULI, J.; ONKEN, U. (1994), "Determination of local hydrodynamic parameters in bubble columns by the electrodiffusion method with oxygen as depolarizer", *Journal of Applied Electrochemistry*, vol. 24, July, p. 666-669.
31. SATO, Y., SEKOGUCHI, K. (1975), "Liquid Velocity Distribution in Two- Phase Bubble Flow", *Int. J. Multiphase Flow*, vol. 2, p. 79-95.
32. SCHLICHTING, H. (1963), "Boundary Layer Theory", McGraw-Hill Book Co. Inc. 6th edition.
33. SERIZAWA, A., KATAOKA, T., MICHİYOSHI, I. (1973), "Turbulent Structure of Air-Water Bubbly Flow (I) and (II)", *Proc. 1973 Ann. Meet. At. Energy Soc. Japan*.
34. SERIZAWA, A., KATAOKA, I., MICHİYOSHI, I. (1975), "Turbulent Structure of Air-Water Bubbly Flow II. Local Properties", *Int. J. Multiphase flow*, vol. 2, p. 235-246.
35. SHIRES, G. L., RILEY, P. J. (1966), "The Measurement of Vertical Voidage Distribution in Two-Phase Flow by Isokinetic Sampling." *A. E. E. W.*, M 650.
36. SOOKHAK Lari, K., VAN Reeuwijk, M., and MAKSIMOVIC, Č. (2013). "The role of geometry in rough wall turbulent mass transfer". *Heat and Mass Transfer journal*, 10.1007/s00231-013-1165-4, 1191-1203.
37. TRAVIS, J. R., BURH, H. O., SESONSKE, A. (1971), "A Model for velocity and Eddy Diffusivity Distributions in Fully Turbulent Pipe Flow". *The Canadian J. of Chem. Eng.*, vol. 49, Feb, p. 14-18.
38. TRINH, N. D. (1986), "Experimental and Numerical Predictions of Turbulent Two-Phase Flow Parameters". Ph. D. Thesis, École Polytechnique de Montréal, University .of Montréal, Québec, Canada.
39. VASSALO, P. F.; TRABOLOD, T. A.; MOORE, W. E.; KIROUAC, G. J. (1993), "Measurement of velocities in gas-liquid two-phase flow using Laser Doppler velocimetry", *Experiments in Fluids*, vol. 15, Iss0.3, Aug., p. 227-230.
40. ZIGAMI, T., KATAOKA, I., SERIZAWA, A., MICHİYOSHI, I. (1974), "Liquid Velocity Measurement in Two-Phase Flow Using a Pitot Tube", *fall meet of the Atomic Energy Society of Japan*, E. 13, p. 195.
41. MORGAN R. G., C. N. MARKIDES, C. P. Hale, G. F. Hewitt (2012), "Horizontal liquid-liquid flow characteristics at low superficial velocities using laser-induced fluorescence", *International Journal of Multiphase Flow* 43, 101-117.
42. MORGAN R. G., C. N. MARKIDES, I. Zadrazil, G. F. Hewitt (2013), "Characteristics of Horizontal Liquid - Liquid Flows in a Circular Pipe using Simultaneous High-Speed Laser-Induced Fluorescence and Particle Velocimetry", *International Journal of Multiphase Flow* 49, 99-118.
43. KALPAKLI A., Experimental study of turbulent flows through pipe bends (2012). Technical Reports from Royal Institute of Technology KTH Mechanics SE-100 44 Stockholm, Sweden.

44. SHUSSER M. and M. GHARIB (2002). On the Effect of Pipe Boundary Layer Growth on the Formation of a Laminar Vortex Ring Generated by a Piston/ Cylinder Arrangement Theoret. *Comput. Fluid Dynamics* 15: 303–316.
45. FOX R.W., A. T. MCDONALD and P. J. PRITCHARD (2004). *INTRODUCTION TO FLUID MECHANICS SIXTH EDITION*.
46. Morgan. RG, Markides. CN, Zadrazil. I, Hewitt. GF (2013). Characteristics of horizontal liquid–liquid flows in a circular pipe using simultaneous high-speed laser-induced fluorescence and particle velocimetry. *International Journal of Multiphase Flow* 49, 99-118.
47. Morgan. RG, Ibarra. R, Zadrazil. I, Matar. OK, Hewitt. GF, Markides. CN (2016). On the role of buoyancy-driven instabilities in horizontal liquid–liquid flow, *International Journal of Multiphase Flow*.